ORIGINAL ARTICLE

Characterizing the impact of projected changes in climate and air quality on human exposures to ozone

Kathie L. Dionisio[1], Christopher G. Nolte[1], Tanya L. Spero[1], Stephen Graham[2], Nina Caraway[1,3], Kristen M. Foley[1] and Kristin K. Isaacs[1]

The impact of climate change on human and environmental health is of critical concern. Population exposures to air pollutants both indoors and outdoors are influenced by a wide range of air quality, meteorological, behavioral, and housing-related factors, many of which are also impacted by climate change. An integrated methodology for modeling changes in human exposures to tropospheric ozone (O_3) owing to potential future changes in climate and demographics was implemented by linking existing modeling tools for climate, weather, air quality, population distribution, and human exposure. Human exposure results from the Air Pollutants Exposure Model (APEX) for 12 US cities show differences in daily maximum 8-h (DM8H) exposure patterns and levels by sex, age, and city for all scenarios. When climate is held constant and population demographics are varied, minimal difference in O_3 exposures is predicted even with the most extreme demographic change scenario. In contrast, when population is held constant, we see evidence of substantial changes in O_3 exposure for the most extreme change in climate. Similarly, we see increases in the percentage of the population in each city with at least one O_3 exposure exceedance above 60 p.p.b and 70 p.p.b thresholds for future changes in climate. For these climate and population scenarios, the impact of projected changes in climate and air quality on human exposure to O_3 are much larger than the impacts of changing demographics. These results indicate the potential for future changes in O_3 exposure as a result of changes in climate that could impact human health.

INTRODUCTION

The impact of climate change on human and environmental health is of growing importance given historical and anticipated changes in surface temperatures, weather patterns, precipitation, and possibly extreme weather events. The air quality, human and ecosystem exposures to pollution, and human and ecosystem physiological response to pollutants are expected to be altered as a result of changing climate. Recent integrated climate and air quality modeling studies have demonstrated the potential for climate-driven concentration increases in tropospheric ozone (O_3) in the Southeast United States,[1] O_3 and/or fine particulate matter ($PM_{2.5}$) concentrations throughout the United States,[2] and O_3 in the western United States.[3] In addition, while several previous studies have evaluated the potential for changes in health impacts resulting from climate-influenced changes to ambient US concentration levels,[4–8] to our knowledge none to date have investigated the impact climate change may have on the levels of air pollutants to which individuals could be exposed.

Human population exposures to air pollutants both indoors and outdoors can be influenced by a wide range of factors in addition to regional-scale concentrations, including local-scale meteorology, human behavior and mobility, land-use, spatial patterns of population density, and housing characteristics, each of which can also be affected by changes to climate. As ambient concentrations can exhibit significant spatiotemporal variability,[9,10] modeled population metrics of exposure (such as population medians or

the number of individuals experiencing exposure above a threshold) can be impacted not only by the magnitude of the concentrations but also by where people spend time (e.g., indoors or outdoors), where they live (e.g., urban or suburban settings), and other behaviors (e.g., window opening and air conditioner use).[11,12] In addition, these exposures are influenced by the infiltration of ambient pollutants into residential and other indoor environments, which is driven (at least in part) by the rate at which the indoor air volume overturns (i.e., air exchange rates (AERs)).[13] AERs, in turn, may depend on climate-sensitive factors, such as indoor/outdoor temperature differentials (i.e., stack effects)[14,15] and use of air conditioning and window opening.[16] Human exposure modeling methods used by the US EPA for assessments in support of the National Ambient Air Quality Standards (NAAQS)[17] incorporate such human activity and housing considerations into population exposure estimates. In addition, these methods use spatially resolved census data to generate simulated individuals,[18,19] allowing for assessment of population magnitude and location shifts. By considering potential climate-related changes in these various factors, we model spatially resolved exposure impacts resulting from potential climate change scenarios and quantify the contribution of each factor to the magnitude of the impacts.

Here we focus on investigation of O_3, given the degree of health concern at its existing ambient concentration levels, the potential for increasing emissions of O_3 precursors with increasing population density in and around urban areas, and the increases

[1]National Exposure Research Laboratory, Office of Research and Development, U.S. Environmental Protection Agency, Research Triangle Park, North Carolina, USA and [2]Office of Air Quality Planning and Standards, U.S. Environmental Protection Agency, Research Triangle Park, North Carolina, USA. Correspondence: Dr. Kathie L. Dionisio, U.S. EPA, 109 T.W. Alexander Drive, Mail Code: E205-02, Research Triangle Park, NC 27709, USA.
Tel.: +1 919 541 1321. Fax: +1 919 541 0329.
E-mail: dionisio.kathie@epa.gov
[3]Current address: CDM Smith, Raleigh, North Carolina, USA.

in temperature that would tend to increase the number of days in a year having meteorological conditions favorable to O_3 formation.[20] In 2015, the US EPA revised its health-based NAAQS for O_3, lowering it from 75 p.p.b to 70 p.p.b (daily maximum 8-h (DM8H) concentration), largely based on the expected increase in public health protection associated with that new concentration level for at-risk populations, particularly children and asthmatics.[17,21]

In this manuscript, we demonstrate the utility of linking existing modeling tools to assess the potential impacts of climate change on population exposure to O_3 using an integrated modeling system that accounts for potential changes in ambient air quality following projected scenarios of climate change. Further, we integrate socio-demographic scenarios (changes in population distribution, fertility, and migration) related to a range of potential future emission pathways. We examine comparisons of population distributions of O_3 exposure for multiple scenarios of potential changes in future climate and demographics.

METHODS
An integrated methodology for estimating changes in human exposures to O_3 owing to future changes in climate and population demographics was developed by linking existing modeling tools for climate, weather, air quality, population distribution, and human exposure (Figure 1). Steps involved in the integrated methodology are described below.

The US EPA's Air Pollutants Exposure Model (APEX) version 4.5 (model available for download at https://www.epa.gov/fera/download-trimexpo-inhalation-apex) was used to perform the human exposure modeling analysis.[18,19] In this analysis, 12 major metropolitan areas of the United States were analyzed. These areas were defined by their Combined

Statistical Area (CSA), and each includes between 5 and 50 counties. The 12 cities were a subgroup of study areas used in the 2014 NAAQS Health Risk and Exposure Assessment for O_3,[17] effectively representing a range of geographic areas, with diverse urban population demographics, varying climate, and ambient O_3 concentrations that were $\geqslant 75$ p.p.b, the standard at that time. DM8H human exposures to O_3 were analyzed for the ozone season (i.e., months conducive to O_3 formation) specific to each CSA as defined in the Code of Federal Regulations for ambient air quality surveillance[21] (Figure 2). A simulated population of 25,000 individuals for each CSA was modeled, with results presented for the entire population and also for children, defined as ≤18 years of age. Details of the development of climate, air quality, and population data for input to APEX for current and future climate change scenarios, and application of the model, are described in the following sections.

Regional Climate and Air Quality
To simulate the effects of climate change on air quality, global climate fields from the Community Earth System Model (CESM)[22] simulations conducted for the fifth phase of the Coupled Model Intercomparison Project (CMIP5)[23] were dynamically downscaled to 36×36 km^2 using the Weather Research and Forecasting (WRF) model.[24] The dynamical downscaling techniques used in WRF have been described previously.[25,26] The WRF model generated hourly meteorological data over North America for four 11-year periods: the years 1995–2005 (hereinafter 2000, or base case (BC$_{clim}$)) from the CMIP5 historical twentieth century experiment, and the years 2025–2035 (hereinafter 2030) following three Representative Concentration Pathways (RCPs).[27] The data for the future period (i.e., 2030) are assumed to be equally plausible in any given year around 2030 following that climate scenario. The three RCPs downscaled here are RCP 4.5, RCP 6.0, and RCP 8.5. In the name of each RCP, the number indicates the radiative forcing in Watts/m^2 at the year 2100, such that the higher RCPs are more extreme global warming pathways. However, owing to
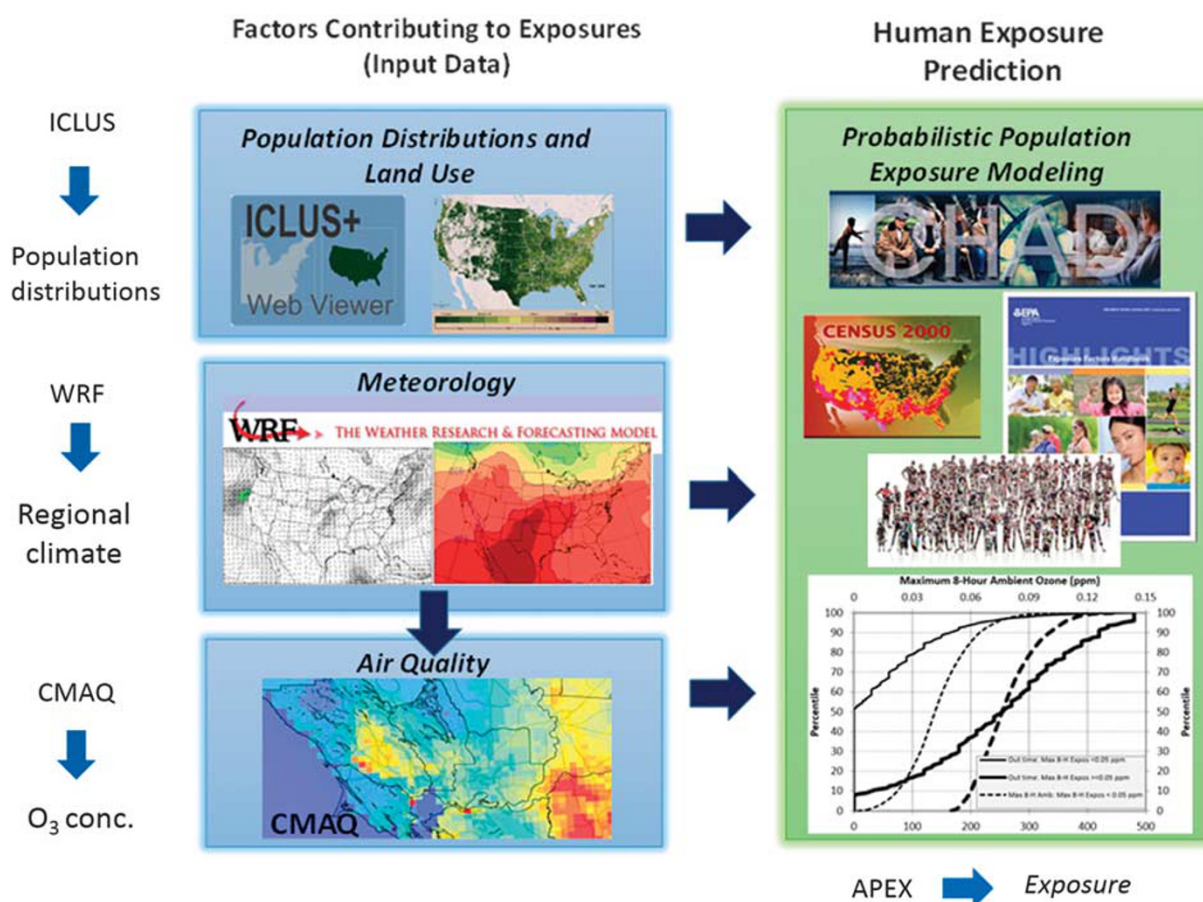

Figure 1. Integrated modeling system.

CSA	Study Area (Abbreviation)	O$_3$ Season
122	Atlanta (ATL)	Mar 1-Oct 31
148	Boston (BOS)	Apr 1-Sep 30
176	Chicago (CHI)	Apr 1-Oct 31
184	Cleveland (CLE)	Apr 1-Oct 31
220	Detroit (DET)	Apr 1-Sep 30
288	Houston (HOU)	Jan 1-Dec 31
348	Los Angeles (LAX)	Jan 1-Dec 31
408	New York (NYC)	Apr 1-Oct 31
428	Philadelphia (PHI)	Apr 1-Oct 31
472	Sacramento (SAC)	Jan 1-Dec 31
476	St. Louis (STL)	Apr 1-Oct 31
548	Wash., DC (WAS)	Apr 1-Oct 31
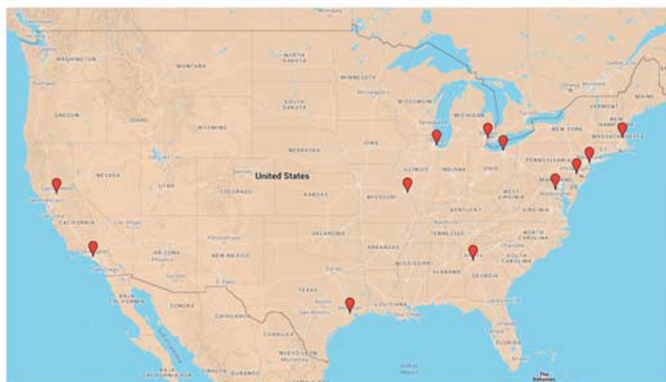
Figure 2. Ozone (O$_3$) seasons by metropolitan study area.

Table 1. Assumptions surrounding demographic models used to obtain future population projections (data from Table 3-1 in US EPA[30]).

Storyline	Fertility	Domestic migration	Net international migration
A1	Low	High	High
B1	Low	Low	High
A2	High	High	Medium
B2	Medium	Low	Medium
Base case (BC$_{pop}$)	Medium	Medium	Medium

Table 2. Scenario pairings modeled with APEX.

		Population						
		BC$_{pop}$			A1	A2	B1	B2
Climate		2010	2030	2100	2100	2100	2100	2100
BC$_{clim}$	1995–2005	X	X	X	X	X	X	X
RCP 4.5	2025–2035		X					
RCP 6.0	2025–2035		X					
RCP 8.5	2025–2035	X	X					

regional and climatic variability, any given year prior to 2100 in a cooler scenario may be warmer for a particular region than the corresponding year in a hotter scenario, particularly early in the twenty-first century, when the degree of divergence between the scenarios is less pronounced.

The downscaled meteorology was used with the Community Multiscale Air Quality (CMAQ) model[28] to simulate air pollutant concentrations at a 36×36 km^2 scale over the conterminous United States. A 2030 emission inventory was used for both the historical and future climate periods, so that the climate impacts on air quality in each scenario could be isolated from policy-driven emissions changes. Additional details of the CMAQ modeling configuration can be found elsewhere.[4] Hourly temperature and O$_3$ concentrations for the 12 metropolitan regions of interest were extracted from the grid cells of the WRF and CMAQ simulations that were the closest match to each of the census tract centroids within each CSA.

Population Projections

Future projections of US population distribution were obtained from the US EPA's Integrated Climate and Land-Use Scenarios (ICLUS) project.[29] In the ICLUS model, social, economic, and demographic storylines from the Intergovernmental Panel on Climate Change's Special Report on Emissions Scenarios (SRES) were adapted for the United States.[30] ICLUS provides geographically explicit population projections for four storylines reflecting different assumptions about changes in future fertility, mortality, and immigration based on the adapted SRES storylines, in addition to a base case scenario. Assumptions around each of the four storylines (A1, B1, A2, B2, and base case (BC$_{pop}$)) are presented in Table 1 and further defined in US EPA.[30] For each storyline, detailed population projections

were available for each decade from 2010 through 2100 inclusive, for five race/ethnicity groupings, by sex, by age (yearly from 0–99), and by Federal Information Processing Standard (FIPS) county code. For more information on ICLUS, and to download the population projections used in this analysis (ICLUS Tools and Datasets Version 1.3.2), see the EPA's website.[31]

Human Exposure

APEX version 4.5 was used to model human inhalation exposures to O$_3$ for the 12 US metropolitan areas. This probabilistic model simulates the movement of individuals through space and time and their resulting exposure in each microenvironment visited. Inputs to the APEX model were the outdoor ambient air quality estimates output from the CMAQ model, corresponding meteorological conditions output from the WRF model, future projections of US population distributions from ICLUS, and existing human time–location–activity patterns from the current version of US EPA's Consolidated Human Activity Database (CHAD),[32,33] available at (https://www.epa.gov/healthresearch/consolidated-human-activity-database-chad-use-human-exposure-and-health-studies-and). CHAD survey data are used to develop a continuous time series of the locations simulated individuals may visit, the activities performed, the time of day these events occur, and their durations. Because the CHAD data are actual records of human activity patterns, they fulfill an essential need of this investigation, that is, realistically representing when time spent outdoors corresponds with the highest O$_3$ concentrations that could occur throughout a day.[17] Notably, for this analysis, CHAD diaries are grouped into temperature bins representing average temperature on the day where activity was recorded. Selection of representative human activity patterns in our modeling includes matching of average daily temperature for the
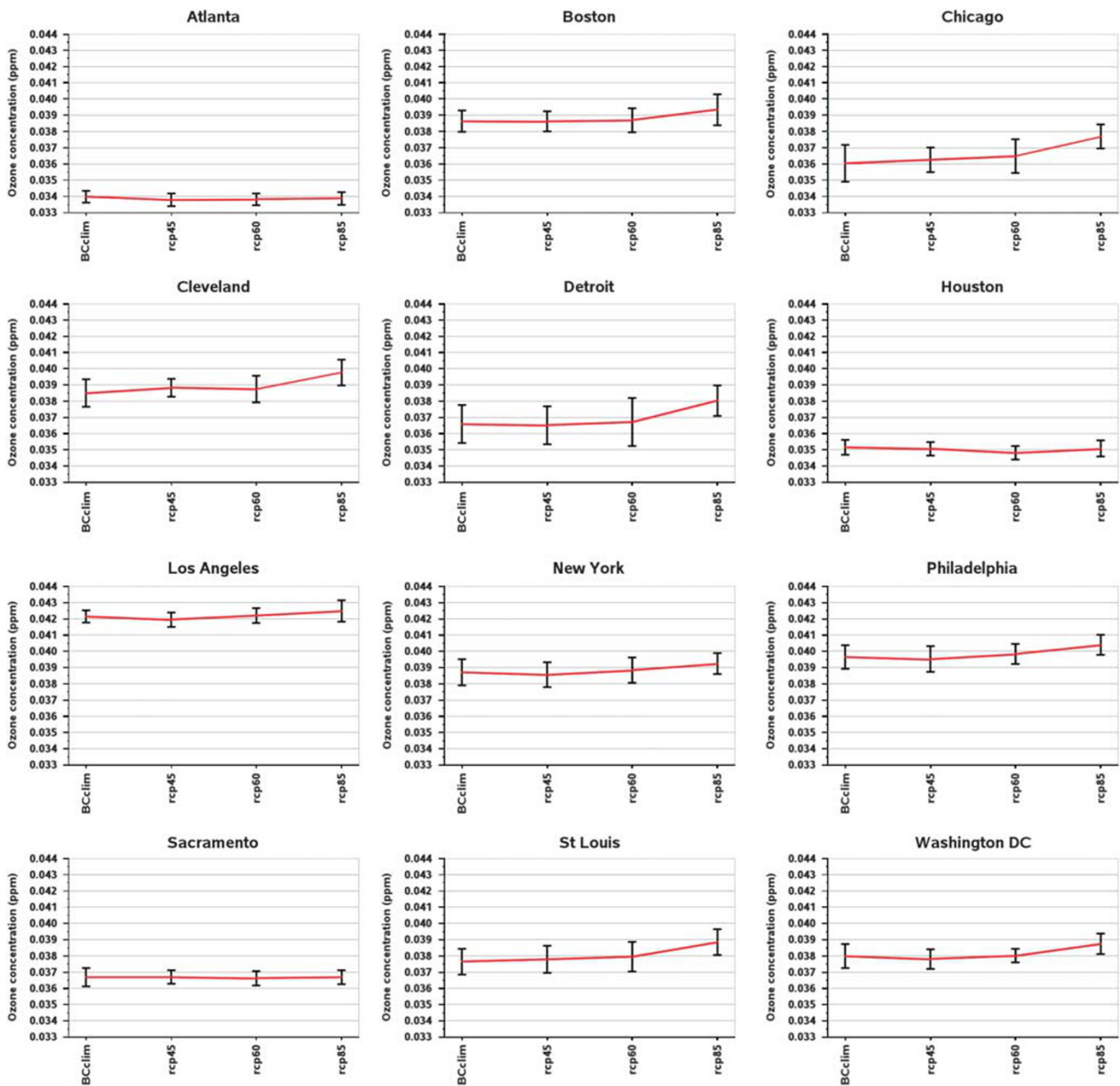
Figure 3. Mean O$_3$ concentrations by city and climate scenario, for city-specific O$_3$ seasons. Error bars represent SD of the means over the 11 representative years.

desired future day with a diary from the appropriate temperature bin in CHAD, to ensure that temperature-dependent human activities are correctly accounted for. Additional inputs to APEX include employment probabilities stratified by sex and age group from the 2000 US census, aggregated to county FIPS code, and baseline physiological data by age and sex. Other city-specific and global APEX inputs not described herein (e.g., employment probabilities, physiological data by age and sex) were the same as those used in the recent NAAQS O$_3$ exposure assessment.[17]

Scenarios Modeled

All comparisons of population exposure used the same CHAD, employment, and baseline physiological data for model input, as these were assumed to be constant over the period of climate projection. Owing to the large number of possible combinations for future climate and

population scenarios, a sampling of combined population and climate pairings were used as key inputs to APEX (Table 2), focusing on varying climate projections for the base case population and varying population projections for the base case climate conditions. For the future climate projections, the 11 available years represent equally likely sets of meteorology and corresponding air quality concentrations, thus all 11 climate years were modeled in each population–climate scenario pairing chosen. The APEX model was run separately for each of the 12 metropolitan areas, for each population–climate pairing. The population projections for 2100 were often chosen for modeling runs to represent the most extreme case of demographic change in the population, as the decade-interval population projections represent more gradual changes. In other cases, the 2010 or 2030 population projections were chosen to more closely match the year of the climate projections.
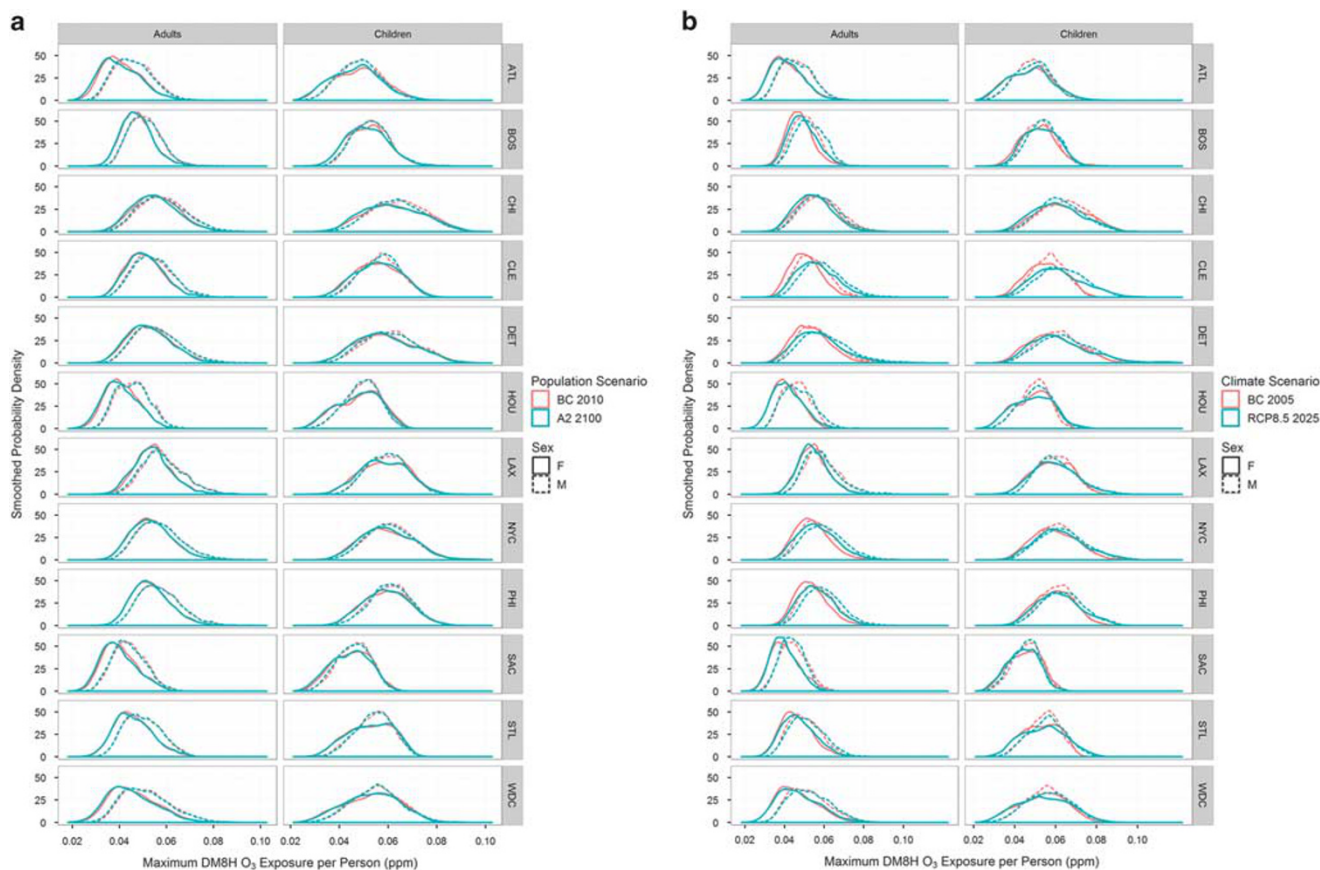
Figure 4. Distributions of individual yearly maximum of DM8H O₃ exposure by city. (**a**) BC_{clim} 2005. (**b**) BC_{pop} 2010.

Exposure Metrics and Statistical Analysis

The APEX model estimates the time series of exposure to O₃ for each simulated individual. APEX can calculate numerous time-averaged exposure metrics of interest (e.g., 5 min, 1 h, etc.). Here the DM8H O₃ exposure was chosen to correspond to controlled human exposure studies that demonstrate adverse health effects resulting from 6- to 8-h O₃ exposures.[21,34] The estimated DM8H O₃ exposures were compared against thresholds of 60, 70, and 80 p.p.b., consistent with the levels selected as part of the most recent O₃ NAAQS review.[17,34]

Probability density function (PDF) plots and cumulative distribution function (CDF) plots were created to examine baseline differences in the population distribution of each individual's maximum DM8H exposure over a calendar year. PDF plots allow for comparison by sex, age (adult *vs* children (≤18 years)), and city, while CDF plots allow for easier comparison between two different scenarios. Bar charts were created for comparison of the percentage of the population in each city, by age, with at least one exceedance (i.e., at least one DM8H exposure that is above the threshold) in a calendar year; city-specific comparisons were made for population changes (holding climate constant) and for varying climate scenarios (holding population constant).

All 11 equally representative years for each climate scenario were run through the APEX model and annual exceedance counts were averaged over the 11 runs. We summarize persons with at least three exceedance days per year, for each concentration threshold analyzed. The percentage change (increase or decrease) in the count of individuals with at least three exceedances for various potential future climate or population scenarios is defined as:

$$\% \text{ change} = \left(\frac{\text{count for future case} - \text{count for baseline case}}{\text{count for baseline case}} \right) \times 100.$$

The 'at least three' exceedances value was chosen to allow for examination of individuals who have repeated exposures above each threshold, in addition to the comparisons described above for individuals with at least one exposure above threshold.

RESULTS

Predicted O₃ Air Concentrations

CMAQ was used to predict spatially resolved ambient O₃ concentrations for the continental United States (on a $36 \times 36 \text{ km}^2$ grid) for the historical base case climate scenario (BC_{clim}) and RCPs 4.5, 6.0, and 8.5. Eleven representative years were simulated for BC_{clim} (1995–2005) and each RCP (2025–2035) as described in Methods. Detailed O₃ results for RCP 8.5 (the most extreme RCP) have previously been reported[4]; results (average change from BC_{clim}) for all three RCP scenarios for the period May–September are shown in Supplementary Figure S1. On average, at 2030 we see the most dramatic increase in concentrations in Siouxland (where Minnesota, Nebraska, Iowa, and South Dakota meet), in the Cleveland, Ohio/Lake Erie/Lake Ontario area, and in the New York to Virginia stretch of the East Coast (Supplementary Figure S1). Mean O₃ concentrations were calculated for each city over its individual O₃ season (see Figure 2) for BC_{clim} and each RCP (Figure 3). Census-tract-level concentrations were equally weighted in calculating the city means; the plotted error bars illustrate the SD of the means over the 11 representative years (e.g., 2025–2035 for the RCP scenarios). LAX had the highest overall absolute O₃ concentrations over its season (42–43 p.p.b), while ATL had the lowest. In general, the differences in city mean between BC_{clim} and RCPs 4.5 and 6.0 were of similar magnitude as the year to year variability in O₃ concentration, while the magnitude of the impact at RCP 8.5 varied across cities. Consistent with the United States May–September results, DET, CHI, CLE, and STL had the largest increases (compared with BC_{clim}) in mean O₃-season concentrations, while smaller increases were also observed in BOS, PHI, and WDC.
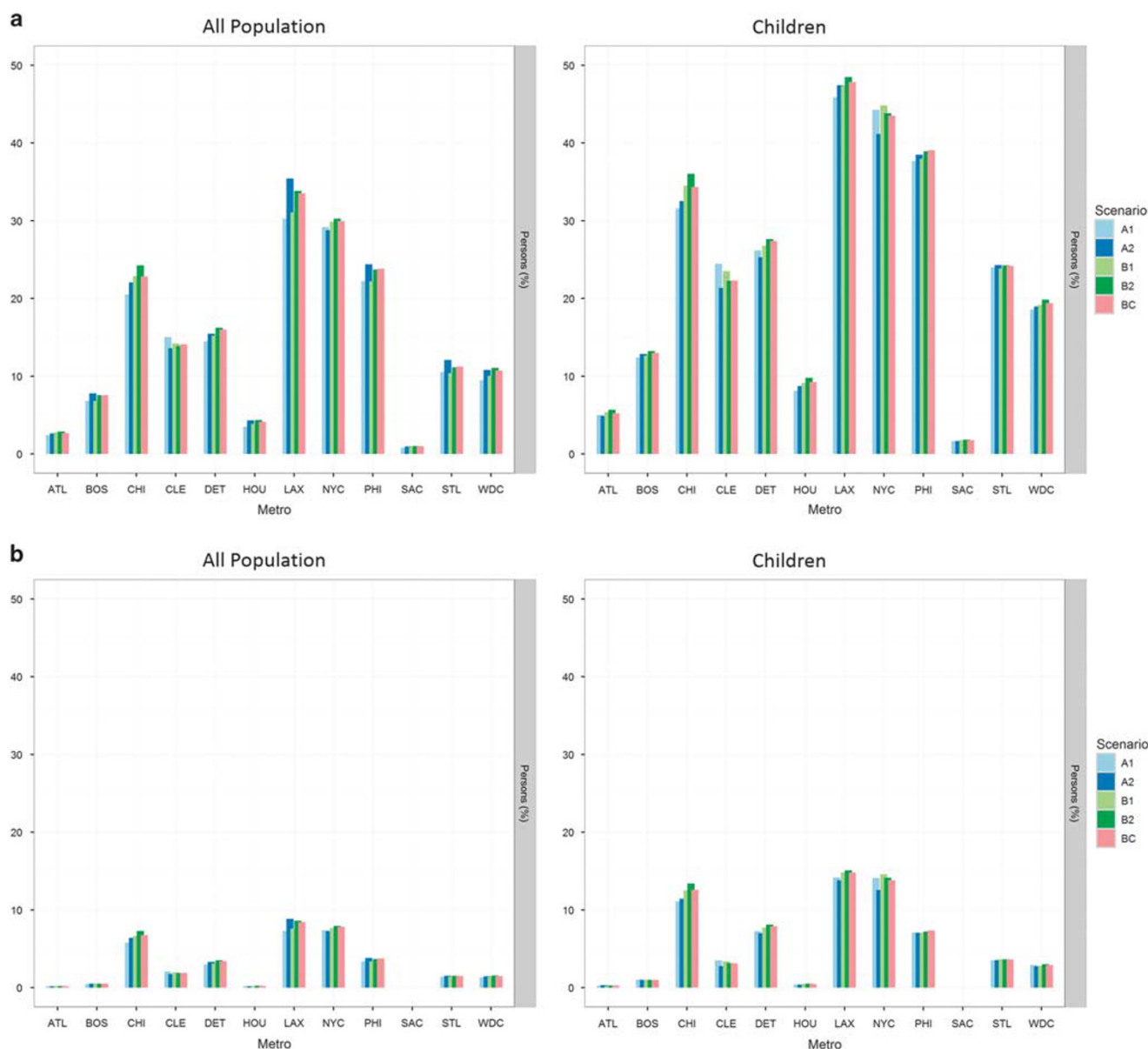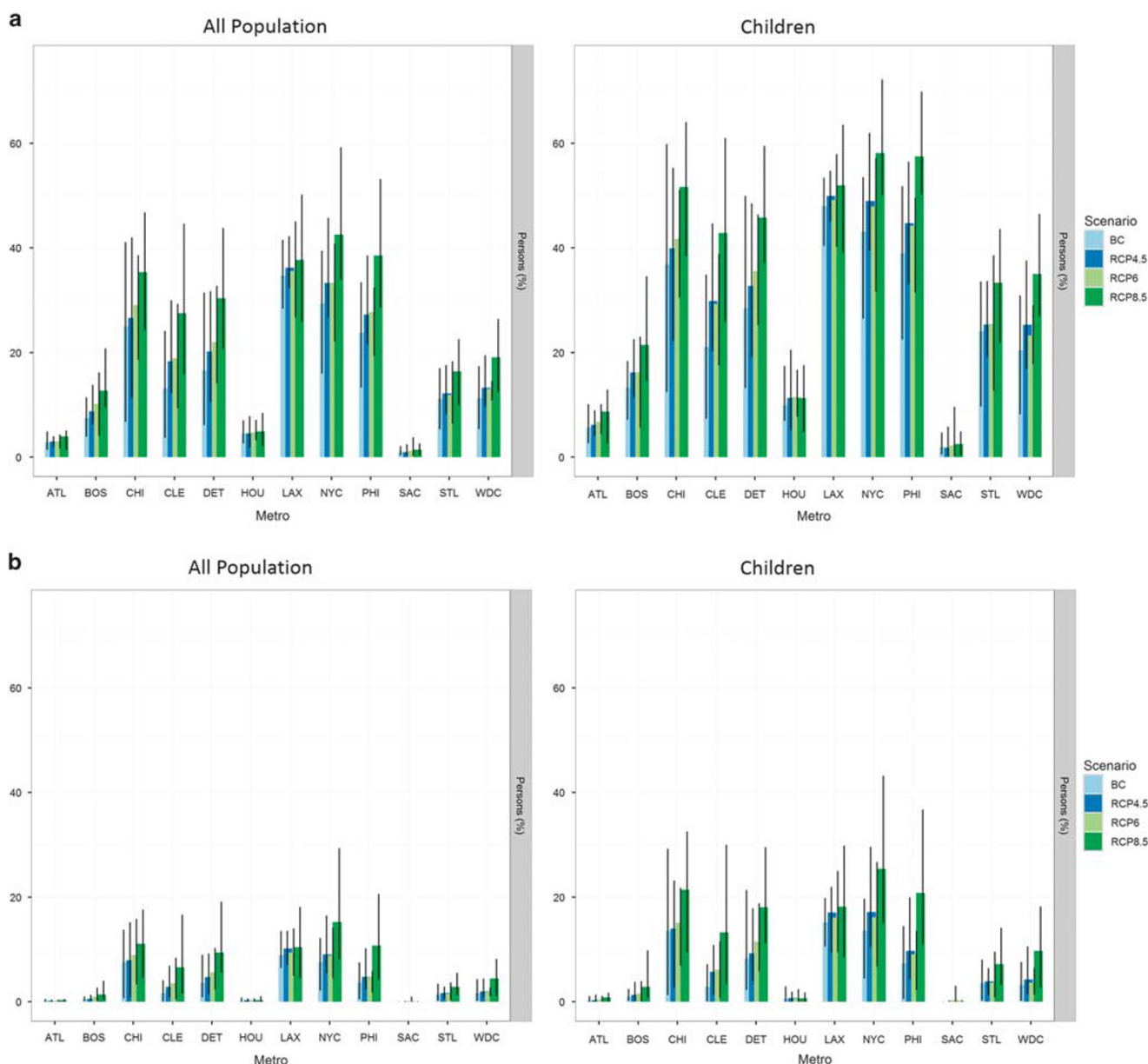
Figure 5. Percentage of population with at least one DM8H exposure above threshold by comparison across population scenarios. (**a**) 60 p.p.b exposure threshold. (**b**) 70 p.p.b exposure threshold.

Predicted O$_3$ Exposures

Although spatial trends in air quality provided evidence of climate-based increases in O$_3$ concentrations in some regions of the United States (especially for RCP 8.5), consideration of spatial distribution of the population and spatiotemporal patterns in infiltration are also required to quantify exposure (and thus potential health) impacts. Overall, APEX exposure modeling results show differences in population distributions of exposure to O$_3$ when comparing different future climate scenarios but show minimal differences from projected changes in demographics and geographic distribution of the population. The left panels of Figure 4a and b show baseline differences in the population distribution of individual adult's annual maximum DM8H exposure by age, sex, and city (i.e., differences for the current population and climate scenario). Figure 4 and Supplementary Figure S2 show a representative year from the 11 climate years, for illustration. As an example of the variability present from the 11 climate years, for

adult females with the median exposure of 39 p.p.b. in ATL, the standard deviation of their exposures across the 11 climate years ranges from 3 p.p.b. to 6 p.p.b. In the total population, differences in exposure by sex are significant, with men overall having a greater incidence (i.e., curve shifted to the right) of high exposures than women. Differences by sex are also seen for children (right panel of Figure 4a and b), often with the peak (mode) DM8H exposure being greater for male compared with female children (likely driven by greater time spent outdoors for male children). DM8H exposures for children also tend to be greater than those estimated for the total population at the mid to upper percentiles of the distribution, indicating that children experience exposures of concern more frequently than adults. Beyond these general comparisons, city specific differences are evident. PDF distributions in Figure 4 show the relatively low percentage of individuals with O$_3$ exposures exceeding 80 p.p.b; for this reason data are not presented at this threshold.

Figure 6. Percentage of population with at least one DM8H exposure above threshold by comparison across climate scenarios. Black lines represent the range (min. to max.) of the percentage of the population having at least one exceedance over the 11 modeled years. Thus the black lines represent the variability in the percentage of the population with at least one exceedance that comes solely from the interannual variability in ozone air quality owing to meteorology. (**a**) 60 p.p.b exposure threshold. (**b**) 70 p.p.b exposure threshold.

To examine the most extreme case of demographic changes, we hold climate constant (BC$_{clim}$ 2005) and compare exposures for the base case population scenario (BC$_{pop}$ 2010) with the most extreme scenario for population change (A2 2100) (Figure 4a). Comparison of exposures from the two different population scenarios shows that even in the case of the most extreme demographic change, we see minimal differences in the proportion of the population experiencing particular exposures across the full distribution of DM8H exposure levels. In comparison, when we hold population constant (BC$_{pop}$ 2010) and examine differences for the most extreme change in climate (BC$_{clim}$ 2005 *vs* RCP 8.5 2025), we see evidence of substantial changes in maximum exposure, particularly in certain cities (CLE and DET and, to a lesser extent, NYC and PHI) (Figure 4b). Examining the CDF for the same contrast of extreme climate change, we can see the shift in exposure more clearly, with increased maximum DM8H exposures

under the RCP 8.5 scenario compared with the base case (e.g., CDF curve shifts to the right for CLE, DET, NYC, and PHI) (Supplementary Figure S2).

In Figure 5, we examine exposures under all population projections (BC$_{pop}$, A1, A2, B1, and B2) for the year 2100 with year 2000 climate and air quality, using the percentage of the population in each city with at least one DM8H O₃ exposure above a threshold. For comparisons of differences in exposure owing to population changes (holding climate constant), the height of each bar represents the mean percentage of the population with at least one exceedance across the 11 climate years. Exposures under different climate scenarios, holding population constant, are presented in Figure 6.

To examine the most extreme population scenario, we use the projected population demographics for 2100. Figure 5 shows that although there are still city-to-city differences in the percentage of

the population with at least one exceedance per year (i.e., at least one DM8H O$_3$ exposure above the threshold), regardless of the potential changes in future population demographics represented by the A1, A2, B1, and B2 scenarios, we see minimal change in the percentage of the population within each city with at least one exceedance. Specifically, for all population we see a < 6% and < 2% difference between maximum and minimum scenarios in the percentage of the population with at least one exceedance for each city for 60 p.p.b and 70 p.p.b thresholds, respectively, and for children a < 5% and < 3% difference for 60 p.p.b and 70 p.p.b thresholds, respectively. For both the base case and population change scenarios, a larger percentage of children experience an exceedance. This holds true across all three O$_3$ exposure thresholds (60, 70, and 80 p.p.b). By contrast, when using the same metric to examine the percentage of the population having at least one exceedance when population is held constant (BC$_{pop}$ 2030) and climate scenarios are varied (BC$_{clim}$ 2000, and RCPs 4.5, 6.0, and 8.5 2030), larger differences are evident for all population (up to 15% and 8% difference in mean between maximum and minimum scenarios for each city for 60 p.p.b and 70 p.p.b thresholds, respectively) and children (up to 22% and 14% difference in mean for 60 p.p.b and 70 p.p.b thresholds, respectively), particularly for the 60 p.p.b threshold (Figure 6a). The magnitude of impact of future climate scenarios varies by city, with some cities seeing a very small degree of change (e.g., ATL, HOU, LAX, SAC) and others seeing a larger degree of change (e.g., CHI, CLE, DET, NYC, PHI, and to a lesser extent, STL and WDC) (Figure 6a). In those cities which see a larger variation across climate scenarios, the mean percentage of the population with at least one exceedance tends to increase as you move from the base case climate scenario through RCPs 4.5, 6.0, and 8.5. Within Figure 6 it is important to note the black bars, which represent interannual variability in the exceedances modeled using the 11 years in each climate scenario. Though within each city the black bars overlap each other, they still echo the trend seen in the mean percentage of the population with at least one exceedance, which is a trend of increase in individuals experiencing an exceedance as we follow the increasing radiative forcing in future climate scenarios.

In addition to the impact on the percentage of the population with at least one exposure above each threshold, we examine the percentage change in the number of people experiencing at least three exceedances per year compared with the base case, across population and, separately, climate scenarios. For the different future population scenarios, we see relatively small variations in the proportion of the total population having at least three

exceedances > 60 p.p.b O$_3$. In comparison to the base case (BC$_{pop}$), the greatest variation overall occurs in the A1 population scenario, with differences as large as 22% in SAC (see Table 3). The largest changes overall were from comparisons of the A1 population scenario (low fertility, high domestic and international migration) with the base case population scenario BC$_{pop}$ (medium fertility and migration). We note that the comparison of A1 and B1 to the BC$_{pop}$ scenario results, with few exceptions, in decreases in the percentage having exceedances. These decreases are largely driven by the decrease in fertility for the A1 and B1 scenarios, evidenced also by the notable decreases in the percentage of children with at least three exceedances for the A1 and B1 scenarios (Table 3). By contrast, when examining changes in the percentage of the population having at least three exceedances across future climate scenarios, we see up to nearly a 250% increase relative to the year 2000 base case (Table 4). Such dramatic increases in the percentage of people with at least three exceedances are accompanied by large absolute numbers of individuals affected (e.g., 2394 additional people with at least three exceedances per year in PHI at 2030 under RCP 8.5 compared with PHI base case for climate), compared with numbers an order of magnitude lower for future population scenarios.

DISCUSSION
Our analysis shows the impact of projected changes in climate and air quality on human exposure to O$_3$ are much larger than the impacts of changing demographics for these climate and population scenarios. Results show baseline differences in exposure patterns and levels by sex, age, geography, and between cities. A number of these differences can be explained by differences in behavior and patterns of where and how different demographic groups spend their time. Men have higher exposures than women, which can be attributed to men spending a larger percentage of their time outdoors (where O$_3$ levels are higher) than women, according to the CHAD database (Figure 4).[11,36] Similarly, children tend to have a higher mean exposure than the total population, with male children having a higher peak of the PDF curve than female children (Figure 4). We attribute this to children spending a greater portion of their day outdoors compared with adults, with male children spending more time outside than female children.[11,37] Although city-to-city differences in exposure levels and patterns exist even at baseline, as previously stated the change in future ambient O$_3$ concentrations appears to be the driver for changes in exposure.

Table 3. Percentage of (count) change in the number of people with at least 3 exceedances > 60 p.p.b across population scenarios, compared with base case population scenario (BC$_{pop}$).

	All population				Children			
	A1 vs BC$_{pop}$	A2 vs BC$_{pop}$	B1 vs BC$_{pop}$	B2 vs BC$_{pop}$	A1 vs BC$_{pop}$	A2 vs BC$_{pop}$	B1 vs BC$_{pop}$	B2 vs BC$_{pop}$
ATL	− 9% (−4)	0% (0)	+11% (+5)	+9% (+4)	− 32% (−6)	+21% (+4)	− 32% (−6)	+11% (+2)
BOS	− 18% (−37)	+10% (+20)	− 17% (−34)	0% (−1)	− 27% (−22)	+28% (+23)	− 27% (−22)	+4% (+3)
CHI	− 15% (−274)	− 3% (−48)	− 1% (−13)	+9% (+164)	− 34% (−218)	+17% (+107)	− 27% (−172)	+6% (+38)
CLE	+6% (+52)	+5% (+39)	− 1% (−10)	− 1% (−9)	− 13% (−38)	+21% (+63)	− 21% (−63)	− 2% (−5)
DET	− 14% (−145)	+2% (+17)	− 9% (−95)	+2% (+26)	− 31% (−135)	+19% (+80)	− 32% (−139)	0% (−2)
HOU	− 21% (−22)	+4% (+4)	− 6% (−6)	+8% (+9)	− 41% (−23)	+7% (+4)	− 30% (−17)	+7% (+4)
LAX	− 15% (−481)	+10% (+340)	− 11% (−364)	+2% (+63)	− 30% (−357)	+27% (+312)	− 26% (−309)	+2% (+25)
NYC	− 5% (−153)	+1% (+18)	− 3% (−79)	+1% (+38)	− 24% (−232)	+17% (+165)	− 23% (−227)	0% (+3)
PHI	− 13% (−251)	+8% (+140)	− 12% (−231)	− 1% (−15)	− 29% (−212)	+23% (+169)	− 29% (−216)	− 2% (−16)
SAC	− 22% (−2)	+0% (0)	− 22% (−2)	+11% (+1)	0% (0)	0% (0)	0% (0)	0% (0)
STL	− 11% (−62)	+6% (+32)	− 10% (−59)	+1% (+5)	− 29% (−86)	+18% (+55)	− 29% (−87)	0% (−1)
WDC	− 19% (−94)	+6% (+32)	− 11% (−55)	+4% (+18)	− 29% (−60)	+20% (+42)	− 27% (−56)	+5% (+10)

Table 4. Percentage of (count) change in the number of people with at least 3 exceedances > 60 p.p.b across climate scenarios, compared with base case climate scenario (BC$_{clim}$).

	All population			Children		
	RCP 4.5 vs BC$_{clim}$	RCP 6.0 vs BC$_{clim}$	RCP 8.5 vs BC$_{clim}$	RCP 4.5 vs BC$_{clim}$	RCP 6.0 vs BC$_{clim}$	RCP 8.5 vs BC$_{clim}$
ATL	− 13% (−7)	0% (0)	+73% (+40)	− 17% (−4)	+8% (+2)	+92% (+22)
BOS	+29% (+59)	+69% (+141)	+175% (+358)	+31% (+27)	+54% (+47)	+169% (+147)
CHI	+9% (+191)	+21% (+439)	+75% (+1570)	+9% (+68)	+18% (+134)	+77% (+571)
CLE	+69% (+496)	+74% (+528)	+249% (+1785)	+73% (+201)	+65% (+179)	+239% (+658)
DET	+36% (+399)	+55% (+607)	+175% (+1929)	+28% (+130)	+45% (+208)	+133% (+622)
HOU	+23% (+26)	+26% (+30)	+35% (+40)	+37% (+23)	+32% (+20)	+42% (+26)
LAX	+7% (+246)	+7% (+223)	+17% (+594)	+6% (+81)	+6% (+73)	+18% (+229)
NYC	+22% (+607)	+25% (+667)	+89% (+2402)	+26% (+241)	+21% (+202)	+75% (+702)
PHI	+25% (+472)	+23% (+426)	+129% (+2394)	+27% (+205)	+21% (+156)	+105% (+793)
SAC	0% (0)	+10% (+1)	+60% (+6)	0% (0)	+50% (+1)	+100% (+2)
STL	+13% (+75)	+12% (+66)	+92% (+528)	+11% (+34)	+13% (+39)	+89% (+265)
WDC	+31% (+166)	+19% (+103)	+162% (+880)	+41% (+98)	+18% (+44)	+166% (+395)

Across the future climate projections, we see a trend of increasing mean percentage of the population having at least one exceedance per year as we move from the year 2000 climate base case to the year 2030 under RCPs 4.5, 6.0, and 8.5 (Figure 6). Further, though there are differences in the extent of increases between cities, Table 4 shows an almost universal trend across all cities of an increasing percentage of the population with at least three exceedances when comparing 2030 climate scenarios to 2000. We note that the cities having the largest increases in exceedances are the cities with the largest increases in ambient O$_3$ concentrations (Figure 3, Supplementary Figure S1). The cities where we saw the largest increase in exceedances for future climate scenarios were CHI, CLE, DET, NYC, PHI, and to some degree, BOS and WDC. Comparing the areas of largest increase in ambient O$_3$ concentration to the cities modeled using APEX (Figure 2, map), we also note that none of the 12 cities modeled overlap Siouxland, the area with the most dramatic ambient O$_3$ increases, indicating that we may not have captured the cities that may be of most concern in this analysis. Finally, we note that though the trend is toward an increasing number of exceedances under higher global warming scenarios, the interannual variability in ambient O$_3$ concentrations using meteorology downscaled from CESM is carried through to the exposure results from APEX (Figure 6, black bars).

As noted, the future scenarios of population change appear to have minimal impact on O$_3$ exposure across all metrics of exposure assessed. This may be because demographic change is inherently slow, thus even across 100 years the impact of changes in fertility, mortality, and migration may be dwarfed by the scale of change in O$_3$ concentration (noting areas of 3–5 p.p.b increase in O$_3$ concentration in Siouxland) (Figure 3, Supplementary Figure S1). As noted above, though the changes in ambient O$_3$ concentration appear to be driving changes in exposure, there may be additional behavior change in the population that may impact exposure change (in either direction) that is not being captured here. Namely, changes in temperature may have an impact on the behavior of the population, particularly with respect to the amount of time spent outdoors. Owing to the current method for matching temperature-dependent activities in APEX using relatively large temperature bins, the comparatively small changes in temperature modeled by the WRF model may not significantly affect the activity pattern data selected to represent the simulated individuals in the population.

In this work, the influence of climate on both AER and human activity patterns were propagated to the exposures indirectly, that is, both AER and human activity diaries are selectively sampled based on temperature predicted from the climate modeling. However, climate may ultimately impact these factors in more direct ways. For example, time spent outdoors could be influenced by ambient temperatures, precipitation, humidity, extreme weather events, and air quality averting behaviors. AER distributions will be influenced by housing stock turnover, construction rates, distribution of new home types, and heating/cooling methods. Further work can be carried out to more explicitly explore potential impacts of these factors and incorporate results into exposure estimates. For example, mechanistic models of AERs that explicitly incorporate housing and climate factors have recently been integrated into EPA human exposure models[12,38]; these methods will be useful in refining climate-relevant AER predictions.

Results shown have the potential to further inform policy decisions and serve to emphasize the key elements of ozone exposure affected by alternate climate scenarios for consideration by public health professionals as well as regulators. Though we see variability around future exposure scenarios owing to variability in the climate scenarios, the trend of increasing percentage of the population experiencing exposures of concern as the degree of radiative forcing in 2100 increases (i.e., as you move from RCP 4.5 to RCP 8.5) has health implications. Further analysis would need to be undertaken to determine the health impact on particularly sensitive subgroups of the population, including asthmatics, of the increasing level and number of days per year individuals may experience exposures of concern. In addition, future research may include modeling cities located in the area of highest ambient O$_3$ increase (i.e., in Siouxland); based on results presented here we would expect populations living in Siouxland to experience the largest increases in the exposure metrics analyzed. These results would need to be combined with data on the number of people living in this area of the country (cities in Siouxland have a much lower population than, for example, NYC or LAX) to determine the relative public health impact nationwide.

Additional future work could include an alternative approach for modeling human behavior (compared with drawing from historical human activity pattern data), which may allow accounting for behavioral changes owing to smaller differences in temperature. An approach for matching temperature-dependent activities that allowed for finer temperature bins may increase the extent to which behavioral changes impact the modeled exposures. For instance and depending on the geographic area, increases in outdoor temperature may lead an individual to either decrease or increase the amount of time they spend outdoors,

leading to lower or higher O$_3$ exposures, respectively. Alternative approaches to modeling human activity may allow us to represent averting behavior patterns that result from public health campaigns designed to inform those at increased health risk owing to pollutant exposures such as the Air Quality Index.[39] Further, activity patterns could be developed to represent recent cultural changes in activity patterns, such as children spending more time indoors performing technology-based activities and less time outdoors, also potentially impacting exposures. In addition, though climate-driven changes in emissions of hydrocarbons from vegetation were considered in air quality modeling, we did not consider the impact of other climate-sensitive emission sources. In particular, wildfires are projected to become more prevalent in a warmer future, particularly in the western United States, and the associated emissions from wildfires would be expected to increase O$_3$ concentrations downwind.

In conclusion, we note that future changes in climate and associated human exposures have the potential for informing public health assessments, dependent upon future levels of increased radiative forcing, which are shown to increase population-based exposures of concern. This, taken together with analyses showing that, even in the most extreme cases of demographic change, future population change is predicted to have a relatively small impact on O$_3$ exposures, supports the conclusion that future changes in climate and air quality will drive future changes in human exposure to O$_3$.

CONFLICT OF INTEREST

The authors declare no conflict of interest.

REFERENCES

1 Zhang Y, Wang Y. Climate-driven ground-level ozone extreme in the fall over the Southeast United States. *Proc Natl Acad Sci* 2016; **113**: 10025–10030.
2 Garcia-Menendez F, Saari RK, Monier E, Selin NE. U.S. air quality and health benefits from avoided climate change under greenhouse gas mitigation. *Environ Sci Technol* 2015; **49**: 7580–7588.
3 Lin M, Fiore AM, Horowitz LW, Langford AO, Oltmans SJ, Tarasick D *et al*. Climate variability modulates western US ozone air quality in spring via deep stratospheric intrusions. *Nat Commun* 2015; **7105**: 1–11.
4 Fann N, Nolte CG, Dolwick P, Spero TL, Brown AC, Phillips S *et al*. The geographic distribution and economic value of climate change-related ozone health impacts in the United States in 2030. *J Air Waste Manag Assoc* 2015; **65**: 570–580.
5 Post ES, Grambsch A, Weaver C, Morefield P, Huang J, Leung L-Y *et al*. Variation in estimated ozone-related health impacts of climate change due to modeling choices and assumptions. *Environ Health Perspect* 2012; **120**: 1559–1564.
6 Sun J, Fu J, Huang K, Gao Y. Estimation of future PM2.5- and ozone-related mortality over the continental United States in a changing climate: an application of high-resolution dynamical downscaling technique. *J Air Waste Manag Assoc* 2015; **65**: 611–623.
7 Patz JA, Frumkin H, Holloway T, Vimont DJ, Haines A. Climate change: challenges and opportunities for global health. *J Am Med Assoc* 2014; **312**: 1565–1580.
8 Bell ML, Goldberg R, Hogrefe C, Kinney PL, Knowlton K, Lynn B *et al*. Climate change, ambient ozone, and health in 50 US cities. *Climatic Change* 2007; **82**: 61–76.

9 Pearce JL, Waller LA, Sarnat SE, Chang HH, Klein M, Mulholland JA *et al*. Characterizing the spatial distribution of multiple pollutants and populations at risk in Atlanta, Georgia. *Spat Spatiotemporal Epidemiol* 2016; **18**: 13–23.
10 Wade KS, Mulholland JA, Marmur A, Russell AG, Hartsell B, Edgerton E *et al*. Effects of instrument precision and spatial variability on the assessment of the temporal variation of ambient air pollution in Atlanta, Georgia. *J Air Waste Manag Assoc* 2006; **56**: 876–888.
11 Graham SE, McCurdy T. Developing meaningful cohorts for human exposure models. *J Expo Sci Environ Epidemiol* 2004; **14**: 23–43.
12 Baxter LK, Burke J, Lunden M, Turpin BJ, Rich DQ, Thevenet-Morrison K *et al*. Influence of human activity patterns, particle composition, and residential air exchange rates on modeled distributions of PM$_{2.5}$ exposure compared with central-site monitoring data. *J Expo Sci Environ Epidemiol* 2013; **23**: 241–247.
13 Mudakavi JR. *Principles and Practices of Air Pollution Control and Analysis*. I K International Publishing House: New Delhi, India, 2010.
14 Breen MS, Schultz BD, Sohn MD, Long T, Langstaff J, Williams R *et al*. A review of air exchange rate models for air pollution exposure assessments. *J Expo Sci Environ Epidemiol* 2013; **24**: 555–563.
15 Ilacqua V, Dawson J, Breen M, Singer S, Berg A. Effects of climate change on residential infiltration and air pollution exposure. *J Expo Sci Environ Epidemiol* 2015; **27**: 16–23.
16 Isaacs K, Burke J, Smith L, Williams R. Identifying housing and meteorological conditions influencing residential air exchange rates in the DEARS and RIOPA studies: development of distributions for human exposure modeling. *J Expo Sci Environ Epidemiol* 2013; **23**: 248–258.
17 U.S. EPA. *Health Risk and Exposure Assessment for Ozone: Final Report (Contract No.: EPA-452/R-14-004a)*. U.S. Environmental Protection Agency, Office of Air Quality Planning and Standards: Research Triangle Park, NC, USA, 2014.
18 U.S. EPA. *Total Risk Integrated Methodology (TRIM) Air Pollutants Exposure Model Documentation (TRIM.Expo/APEX, Version 4.5), Volume I: User's Guide (EPA-452/B-12-001a)*. US EPA Office of Air Quality Planning and Standards: Research Triangle Park, NC, USA, 2012.
19 U.S. EPA. *Total Risk Integrated Methodology (TRIM) Air Pollutants Exposure Model Documentation (TRIM.Expo/APEX, Version 4.5), Volume II: Technical Support Document (EPA-452/B-12-001b)*. US EPA Office of Air Quality Planning and Standards: Research Triangle Park, NC, USA, 2012.
20 USGCRP, Fann N, Brennan T, Dolwick P, Gamble JL, Ilacqua V, Kolb L *et al*. Chapter 3: Air Quality Impacts. *The Impacts of Climate Change on Human Health in the United States: A Scientific Assessment*. U.S. Global Change Research Program: Washington, DC, USA, 2016; pp 69-98. http://dx.doi.org/10.7930/JOGQ6VP6.
21 Code of Federal Regulations. Title 40: Protection of the Environment. Chapter I Section 50.19: National primary and secondary ambient air quality standards for ozone. 2015.
22 Gent PR, Danabasoglu G, Donner LJ, Holland MM, Hunke EC, Jayne SR *et al*. The Community Climate System Model version 4. *J Climate* 2011; **24**: 4973–4991.
23 Taylor KE, Stouffer RJ, Meehl GA. An overview of CMIP5 and the experiment design. *Am Meteorol Soc* 2012; **93**: 485–498.
24 Skamarock WC, Klemp JB. A time-split nonhydrostatic atmospheric model for weather research and forecasting applications. *J Comput Phys* 2008; **227**: 3465–3485.
25 Otte TL, Nolte CG, Otte MJ, Bowden JH. Does nudging squelch the extremes in regional climate modeling? *J Climate* 2012; **25**: 7046–7066.
26 Spero TL, Nolte CG, Bowden JH, Mallard MS, Herwehe JA. The impact of incongruous lake temperatures on regional climate extremes downscaled from the CMIP5 archive using the WRF model. *J Climate* 2016; **29**: 839–853.
27 van Vuuren DP, Edmonds J, Kainuma M, Riahi K, Thomson A, Hibbard K *et al*. The representative concentration pathways: an overview. *Climatic Change* 2011; **109**: 5–31.
28 Byun DW, Schere KL. Review of the governing equations, computational algorithms, and other components of the Models-3 Community Multiscale Air Quality (CMAQ) modeling system. *Appl Mech Rev* 2006; **59**: 51–77.
29 U.S. EPA. *ICLUS Tools and Datasets (Version 1.3.2)*. U.S. Environmental Protection Agency: Washington, DC, USA, 2010.
30 U.S. EPA. *Land-Use Scenarios: National-Scale Housing-Density Scenarios Consistent with Climate Change Storylines*. U.S. Environmental Protection Agency, National Center for Environmental Assessment: Washington, DC, USA, 2009.
31 U.S. EPA. ICLUS Tools and Datasets (Version 1.3.2) 2013 Available from https://cfpub.epa.gov/ncea/global/recordisplay.cfm?deid = 257306.
32 McCurdy T, Glen G, Smith L, Lakkadi Y. The National Exposure Research Laboratory's Consolidated Human Activity Database. *J Expo Anal Environ Epidemiol* 2000; **10**(Pt 1): 566–578.
33 U.S. EPA. CHAD User's Guide: Extracting Human Activity Information from CHAD on the PC. U.S. Environmental Protection Agency, National Exposure Research Laboratory Contract No.: 309213 2000.
34 U.S. EPA. *Integrated Science Assessment for Ozone and Related Photochemical Oxidants*. National Center for Environmental Assessment-RTP Division, Office of

270

Research and Development, U.S. Environmental Protection Agency: Research Triangle Park, NC, USA, 2013. Report number EPA/600/R-10/076F.

35 U.S. EPA. *Policy Assessment for the Review of the Ozone National Ambient Air Quality Standards*. U.S. Environmental Protection Agency, Office of Air Quality Planning and Standards: Research Triangle Park, NC, USA, 2014. Report number EPA-452/R-14-006.

36 Echols SL, MacIntosh DL, Hammerstrom KA, Ryan PB. Temporal variability of micro-environmental time budgets in Maryland. *J Expo Anal Environ Epidemiol* 1999; **9**: 502–512.

37 Xue J, McCurdy T, Spengler J, Ozkaynak H. Understanding variability in time spent in selected locations for 7-12 year old children. *J Expo Anal Environ Epidemiol* 2004; **14**: 222–233.

38 Baxter LK, Stallings C, Smith L, Burke J. Probabilistic estimation of residential air exchange rates for population-based human exposure modeling. *J Expo Sci Environ Epidemiol* 2016 (doi: 10.1038/jes.2016.49; e-pub ahead of print).

39 Neidell M. Information, avoidance behavior, and health: the effect of ozone on asthma hospitalizations. *J Hum Resour* 2009; **44**: 450–478.

Supplementary Information accompanies the paper on the Journal of Exposure Science and Environmental Epidemiology website (http://www.nature.com/jes)